Journal of Alloys and Compounds 622 (2015) 477–482

Contents lists available at ScienceDirect

Journal of Alloys and Compounds

journal homepage: www.elsevier.com/locate/jalcom

Structural, electrical, and magnetic properties of multiferroic $Bi_{1-x}Gd_xFe_{0.97}Co_{0.03}O_3$ thin films

Xu Xue, Guoqiang Tan *, Wenlong Liu, Hangfei Hao, Huijun Ren

School of Materials Science & Engineering, Shaanxi University of Science & Technology, Xi'an 710021, PR China

ARTICLE INFO

Article history:
Received 29 September 2014
Accepted 12 October 2014
Available online 23 October 2014

Keywords:
Multiferroic
Antiferroelectric
Phase transition
Magnetization
Defect

ABSTRACT

Single-phase $Bi_{1-x}Gd_xFe_{0.97}Co_{0.03}O_3$ (BGFC, $x = 0.04–0.16$) thin films were successfully synthesized by using a chemical solution deposition method. The BGFC thin films exhibit a series of structural phase transitions as a function of Gd composition, accompanied by dramatic changes in the ferroelectric, leakage current and dielectric properties. It has been demonstrated that Gd doping at Bi-site can monotonously decrease the remanent magnetization, mainly due to the gradual decrease in Fe^{2+} content. Weak compress stress favors the ferromagnetism in the BGFC ($x = 0.08$) thin film, which takes a maximum saturation magnetization of 13.2 emu/cm^3 with the smallest coercivity of 120 Oe. At particular composition of $x = 0.12$, the film exhibits rectangular hysteresis loop and sharp polarization current curve, a giant remanent polarization of 101 μC/cm^2 and a small coercive field of 345 kV/cm is observed. This paper reports that rare earth driven ferroelectric to antiferroelectric (AFE) phase transition can be obtained at room temperature in the binary elements codoped BFO thin films. Besides, the defect polarization serves approximatively as the AFE domains blocking the ferroelectric switching.

1. Introduction

Despite the persistent attempts to develop novel singlephase magnetic ferroelectrics, $BiFeO_3$ (BFO) remains the only thermodynamically stable compound exhibiting a simultaneous ferroelectric and antiferromagnetic order far above the room temperature ($T_N \approx 643$ K, $T_C \approx 1100$ K) [1]. At room temperature, BFO crystallizes in a rhombohedral structure (space group $R3c$), containing a network of corner-sharing oxygen octahedra, where Fe^{3+} cations are inside the octahedra and Bi^{3+} cations fill in between the cavities. Calculations of the spontaneous polarization in rhombohedral BFO suggested a value between 90 and 100 μC/cm^2 directed along the $[001]_{hex}$ axis because $6s^2$ lone pairs of electrons of the Bi ions distort the geometry of the FeO_6 octahedra [2], and also the first-principle calculations had suggested a giant polarization of 150 μC/cm^2 along the [001] direction of the tetragonal symmetry [3]. Nevertheless, the complex G-type antiferromagnetic (AFM) structure due to the local spin ordering of Fe^{3+} ions, which counteracts the macroscopic magnetization being observed, seriously limits its practical application in magnetoelectric functionality.

Recent investigations have shown that the magnetization of BFO ceramic and nanoparticle can be effectively improved by simultaneously substitution at Bi- and Fe-site in comparison with the single-site doped sample [4,5]. In the case of the BFO thin film, it has early been demonstrated that rare-earth (RE) doping at Bi-site can monotonously increase the saturation magnetization [6] due to the structural phase transition induced reorientation of magnetic dipoles within the G-type AFM structure [7]. However, a major discrepancy is that RE substituted BFO undergoes a ferroelectric (FE) to antiferroelectric (AFE) to paraelectric (PE) phase transition with the increase in dopant content, where the critical concentrations for both FE–AFE and AFE–PE phase boundaries depend on the ionic radius of the substituting element [8,9]. According to the model proposed by Spaldin and co-workers [10], systematic substitution of Bi by RE dopants may not only distort the cation spacing between the octahedral but also alter the long-range ferroelectric order. The short-range antiparallel interactions of the RE ions results in AFE, which dramatically modifies the local dipole alignments and can gradually nucleate and grow with the increase in RE concentration. For excess RE doping concentrations, the AFE disappears and PE phase appears. Therefore, the generally observed double hysteresis loop with a medium polarization in BFO film is a competition result between the FE phase and the AFE phase. Furthermore, due to the easy formation of the $(V_{O^{2-}})^{\cdot\cdot}$ and $\left(Fe^{2+}_{Fe^{3+}}\right)'$ defects in BFO film, the defect polarization associated with the non-centric distribution of defect dipoles is formed along the spontaneous-polarization orientation and thus provides a

* Corresponding author.
E-mail address: tan3114@163.com (G. Tan).

http://dx.doi.org/10.1016/j.jallcom.2014.10.058
0925-8388/

restoring force to reverse the switched ferroelectric domains after removing the field [11], resulting in a double hysteresis loop.

In the present work, we report on the magnetically active ions (Gd and Co) codoped BFO thin films that exhibit a series of structural phase transitions as a function of Gd composition, accompanied by dramatic changes in the ferroelectric, leakage current and dielectric properties. In particular, instead of an expected gradual increase in magnetization, it has been demonstrated that Gd doping at Bi-site can monotonously decrease the remanent magnetization of the sample. The rationales behind such doping experiments are discussed in detail.

2. Experiment

Multiferroic $Bi_{1-x}Gd_xFe_{0.97}Co_{0.03}O_3$ (BGFC, $x = 0.04–0.16$) thin films were deposited on fluorine-doped SnO_2 (FTO)/glass substrates by using a chemical solution deposition method. For the preparation of the precursor solutions, $Bi(NO_3)_3{\cdot}5H_2O$, $Fe{\cdot}(NO_3)_3{\cdot}9H_2O$, $Gd(NO_3)_3{\cdot}5H_2O$ and $Co(NO_3)_2{\cdot}6H_2O$ were dissolved in 2-methoxyethanol and acetic anhydride (3:1 in volume ratio) based on the compound stoichiometric ratio and solution concentration (0.3 mol/L). Here, 5 mol% of excess Bi was added into the solution to compensate for bismuth loss during the heat treatment. After stirring the solutions for 3 h, stable precursor solutions were obtained. The wet BGFC films were deposited on FTO substrates by spin-coating. Each layer of the film was pyrolyzed at 250 °C for 5 min and then annealed at 550 °C for 10 min using a rapid thermal annealing process under atmosphere for crystallization. Then films with various doping concentrations were free-cooled down to room temperature. Repeating the spin-coating process for 16 times, all the BGFC thin films with thicknesses about 800 nm were obtained. All the thin films were grown at the same deposition condition, and no evidence of impurity phases was detected by the X-ray diffractometer. In order to measure the electrical properties, Au electrodes (with areas of 0.5 mm^2) were deposited on the top surface of the thin film and the FTO substrate by ion sputtering through a metal shadow mask to form a capacitor structure. After annealing at 300 °C for 20 min, the electrodes and the film/substrate could be completely contacted.

The crystal structures of the BGFC thin films were characterized using X-ray diffractometer (XRD) with Cu Kα radiation (Rigaku, D/MAX-2200VPC). Field-emission scanning electron microscope (FE-SEM, Hitachi S4800) was used to detect the surface morphologies and thicknesses of the samples. The chemical states of the films were investigated by using an X-ray photoelectron spectroscopy (XPS, Kratos Ltd., XSAM800). Raman measurement was performed by using a Horiba JY HR800 Raman system equipped with 514.5 nm Ar^+ ion excitation source under air ambient condition at room temperature. Room temperature dielectric response was investigated with Agilent E4980A concise LCR meter. The leakage current densities of the films were investigated by using an Agilent B2901A. The ferroelectric properties were measured by using a TF2000 Ferroelectric Analyzer (aix ACCT). Magnetic properties were measured using superconducting quantum interference device (MPMS-XL-7).

3. Results and discussion

Fig. 1(a) shows the XRD patterns of the BGFC ($x = 0.04–0.16$) thin films and the detected trace from the FTO substrates, confirming the pure polycrystalline structures of the BGFC thin films with obvious (104)/(110) preferred orientation, especially when $x = 0.08$. It can be noted from the enlarged view, as shown in the inset of Fig. 1(a), the diffraction peaks (104) and (110) undergo a shift in 2θ accompanied by a decrease in peak splitting, and the (110) peak becomes stronger than the (104) peak on increasing Gd concentration. This suggests the existence of structural transformations and changes in the lattice constants of the BGFC thin films due to the smaller ionic radius of Gd^{3+} compared with that of Bi^{3+}. The average grain sizes and strains estimated from the XRD patterns [12,13] are shown in Fig. 1(b). The average grain size first decreases, taking minimum value at $x = 0.08$, and then increases with increasing Gd content. The tensile stresses are generated in the BGFC films with $x = 0.04$, 0.12 and 0.16, except for the BGFC ($x = 0.08$) thin film that built up a weak compress stress. The magnitude of the strain depends to some extent on the average grain size.

To further investigate the effects of the Gd doping on the microstructure of the films, surface FE-SEM images and the corresponding cross sectional images are carried out and the results are shown

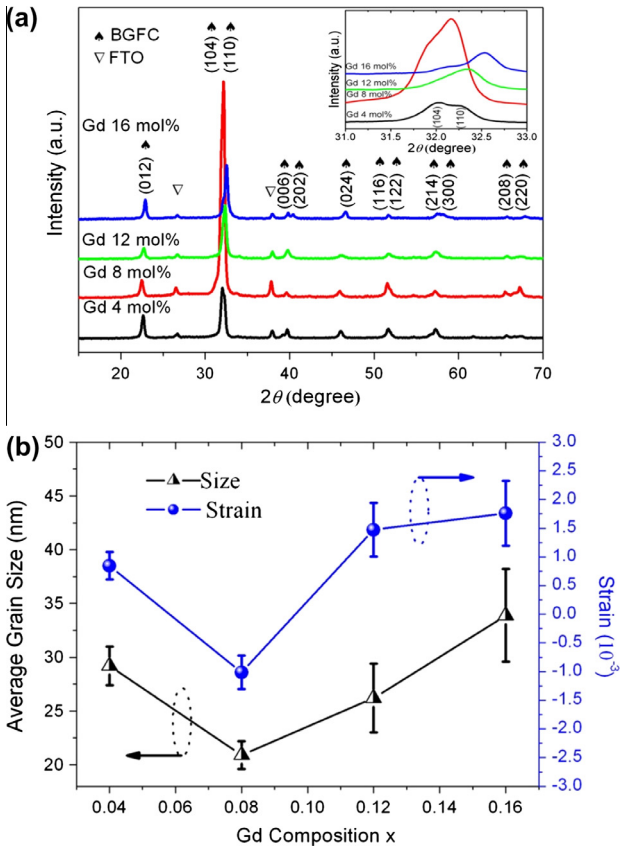

Fig. 1. (a) XRD patterns of the BGFC ($x = 0.04–0.16$) thin films, the right inset is the enlarged part of 2θ around the (104) and (110) peaks. (b) Variation of the average grain size and strain versus Gd concentration.

in Fig. 2(a)–(d). Clear interface layers are observed between the BGFC and FTO layers from the cross sectional FE-SEM images and it can be easily checked that the thicknesses of the films are all about 800 nm. Due to the thermal expansion coefficient misfit and in-plane lattice misfit among the BFO and FTO substrate [14,15], it is inevitable that the tensile stress will generate microcracks and pores in the BGFC thin films during the process of pyrolysis and crystallization. But the big difference in surface morphology between the BGFC ($x = 0.08$) thin film and other samples is that the film is dense, smooth and crack-free, which is consistent with the highest degree of crystallinity and a small compress stress observed in the XRD pattern. This may be probably due to the lattice expansion for the BGFC ($x = 0.08$) thin film, which will result in improving the grain connectivity and densification of the material.

Details of the structure evolution with ion substitution on BFO can be expressed more explicitly through Raman spectra. The room-temperature Raman spectra of the BGFC ($x = 0.04–0.16$) thin films are shown in Fig. 3. According to group theory, the BFO with a rhombohedrally distorted perovskite structure and $R3c$ space group should have 13 ($\Gamma_{opt/R3c} = 4A_1 + 9E$) Raman active modes [16,17], and there are 8 ($3A_1 + B_1 + 4E$) active Raman modes for the tetragonal distorted $P4mm$ space group [18]. In the present study, 10 Raman active modes are identified for the BGFC ($x = 0.04$) thin film, which agrees well with the $R3c$ bulk BFO in terms of relative scattering intensity and mode frequency [19], suggesting the polycrystalline BGFC ($x = 0.04$) thin film grows still with rhombohedral symmetry. As for the BGFC ($x = 0.08$) thin film, the Raman spectra increase in the areas under curve at higher wave numbers and the triclinic ($P1$) structure is strongly suggested